

University of Groningen

An Evaluation of the Fe-N Phase Diagram Considering Long-Range Order of N Atoms in γ' -Fe₄N_{1-x} and ϵ -Fe₂N_{1-z}

Kooi, Bart; Somers, Marcel A.J.; Mittemeijer, Eric J.

Published in:
Metallurgical and Materials Transactions A

DOI:
[10.1007/BF02649775](https://doi.org/10.1007/BF02649775)

IMPORTANT NOTE: You are advised to consult the publisher's version (publisher's PDF) if you wish to cite from it. Please check the document version below.

Document Version
Publisher's PDF, also known as Version of record

Publication date:
1996

[Link to publication in University of Groningen/UMCG research database](#)

Citation for published version (APA):

Kooi, B. J., Somers, M. A. J., & Mittemeijer, E. J. (1996). An Evaluation of the Fe-N Phase Diagram Considering Long-Range Order of N Atoms in γ' -Fe₄N_{1-x} and ϵ -Fe₂N_{1-z}. *Metallurgical and Materials Transactions A*, 27(4). DOI: 10.1007/BF02649775

Copyright

Other than for strictly personal use, it is not permitted to download or to forward/distribute the text or part of it without the consent of the author(s) and/or copyright holder(s), unless the work is under an open content license (like Creative Commons).

Take-down policy

If you believe that this document breaches copyright please contact us providing details, and we will remove access to the work immediately and investigate your claim.

Downloaded from the University of Groningen/UMCG research database (Pure): <http://www.rug.nl/research/portal>. For technical reasons the number of authors shown on this cover page is limited to 10 maximum.

An Evaluation of the Fe-N Phase Diagram Considering Long-Range Order of N Atoms in γ' -Fe₄N_{1-x} and ϵ -Fe₂N_{1-z}

BART J. KOOI, MARCEL A.J. SOMERS, and ERIC J. MITTEMEIJER

The chemical potential of nitrogen was described as a function of nitrogen content for the Fe-N phases α -Fe[N], γ' -Fe₄N_{1-x}, and ϵ -Fe₂N_{1-z}. For α -Fe[N], an ideal, random distribution of the nitrogen atoms over the octahedral interstices of the bcc iron lattice was assumed; for γ' -Fe₄N_{1-x} and ϵ -Fe₂N_{1-z}, the occurrence of a long-range ordered distribution of the nitrogen atoms over the octahedral interstices of the close packed iron sublattices (fcc and hcp, respectively) was taken into account. The theoretical expressions were fitted to nitrogen-absorption isotherm data for the three Fe-N phases. The $\alpha/\alpha + \gamma'$, $\alpha + \gamma'/\gamma'$, $\gamma'/\gamma' + \epsilon$, and $\gamma' + \epsilon/\epsilon$ phase boundaries in the Fe-N phase diagram were calculated from combining the quantitative descriptions for the absorption isotherms with the known composition of NH₃/H₂ gas mixtures in equilibrium with coexisting α and γ' phases and in equilibrium with coexisting γ' and ϵ phases. Comparison of the present phase boundaries with experimental data and previously calculated phase boundaries showed a major improvement as compared to the previously calculated Fe-N phase diagrams, where long-range order for the nitrogen atoms in the γ' and ϵ phases was not accounted for.

I. INTRODUCTION

THE Fe-N phase diagram provides information essential for the practice of nitriding iron and low-carbon steels.^[1] To understand the (in)stability of the Fe-N phases, an appropriate model for the thermodynamics of these phases is required. Preferably, such models for solid phases are based on the crystal lattice of the phase concerned.

Fe-N solid solutions can be conceived as composed of two interpenetrating sublattices: the sublattice for the Fe atoms and the sublattice for the N atoms. The Fe sublattice can be considered to be fully occupied by Fe atoms. The N sublattice, constituted by the octahedral interstices of the Fe sublattice, is partly occupied by N atoms and partly occupied by vacancies V. In α -Fe[N] (bcc Fe sublattice) and also in γ -Fe[N] (fcc Fe sublattice), the nitrogen atoms are distributed more or less randomly over the sites of their own sublattice.^[2,3] In γ' -Fe₄N_{1-x} (fcc sublattice) and in ϵ -Fe₂N_{1-z} (hcp Fe sublattice), the nitrogen atoms show long-range order (LRO) on their own sublattice.^[4-10]

Recently, model descriptions for the thermodynamics of the γ' -Fe₄N_{1-x} and ϵ -Fe₂N_{1-z} phases were presented taking into account the LRO of the nitrogen atoms on their sublattice. The behavior of the nitrogen-absorption isotherms, depicting the dependence of the chemical potential of nitrogen on nitrogen content, was described successfully at several temperatures by using the Gorsky-Bragg-Williams (GBW) approximation for both γ' -nitride and ϵ -nitride.^[11,12,13] From the description of the nitrogen-absorption isotherms of the various Fe-N phases, the corresponding phase boundaries in the Fe-N phase diagram can be calculated straightforwardly

by equating the chemical potentials of nitrogen and of iron for the phases coexisting in equilibrium. For this calculation, knowledge is required of (the differences in) the chemical potentials for the standard state of both nitrogen and iron, $\mu_N^\circ (=G_N^\circ)$ and $\mu_{Fe}^\circ (=G_{Fe}^\circ)$, for the phases concerned. Data for G_N° is available from References 12 and 13; data for G_{Fe}° are not known. In the studies presented so far,^[14-20] values for the difference of G_{Fe}° were evaluated by fitting expressions obtained for the equal chemical potentials of iron in coexisting phases to experimental composition-temperature data for the phase boundary concerned.

Without recourse to experimental phase-boundary data, in the present work, the nitrogen partial pressures pertaining to equilibrium of ammonia/hydrogen mixtures with coexisting α and γ' phases and with coexisting γ' and ϵ phases were used to calculate the $\alpha/\alpha + \gamma'$, $\alpha + \gamma'/\gamma'$, $\gamma'/\gamma' + \epsilon$, and $\gamma' + \epsilon/\epsilon$ phase boundaries in the Fe-N phase diagram from the expressions for the nitrogen-absorption isotherms. The results were compared with existing experimental data for these phase boundaries and with the previous evaluations of the Fe-N phase diagram.

II. CHEMICAL POTENTIAL OF NITROGEN IN FE-N PHASES; NITROGEN-ABSORPTION ISOTHERMS

An equilibrium state of the Fe-N phases γ' -Fe₄N_{1-x} and ϵ -Fe₂N_{1-z} cannot be attained in contact with pure nitrogen gas at atmospheric pressure, because equilibrium partial pressures of nitrogen amount to several GPa's for the iron nitrides (at normal temperatures: 500 to 1000 K). Ammonia/hydrogen gas mixtures at atmospheric pressure are suitable to investigate the thermodynamics of Fe-N phases at atmospheric pressure because of their high virtual nitrogen partial pressure and the wide range of virtual nitrogen partial pressures that can be realized by variation of the ammonia content. Therefore, the Fe-N phase diagram established from data for Fe-N phases in equilibrium with NH₃/H₂ gas mixtures is not the phase diagram of its pure

BART J. KOOI, formerly Graduate Student, Laboratory of Materials Science, Delft University of Technology, is Postdoctoral Student, Materials Science Centre, Department of Applied Physics, University of Groningen, NL-9747 AW Groningen, The Netherlands. MARCEL A.J. SOMERS, Assistant Professor, and ERIC J. MITTEMEIJER, Professor, are with the Laboratory of Materials Science, Delft University of Technology, NL-2628 AL Delft, The Netherlands.

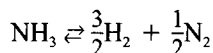
Manuscript submitted June 14, 1995.

components Fe and N₂ at atmospheric pressure.* At at-

*In fact, the diagram usually referred to as the Fe-N phase diagram is a quasibinary Fe-NH₃-H₂ phase diagram or can be interpreted as a projection of data of phase diagrams of Fe and N₂ at various pressures (corresponding with the N₂ partial pressure of the NH₃/H₂ gas mixture holding for a data point).

mospheric pressure, Fe-N phases with an equilibrium nitrogen partial pressure higher than 1 atmosphere tend to decompose into Fe and N₂. Thus, the Fe-N phase diagram obtained from equilibrium studies of Fe-N phases with NH₃/H₂ gas mixtures is a metastable phase diagram (*cf.* the metastable and stable Fe-C phase diagrams).

The chemical potential of nitrogen in a gas phase, $\mu_{N,g}$, consisting of an NH₃/H₂ mixture can be defined on the basis of the hypothetical equilibrium



where

$$\mu_{N,g} \equiv \frac{1}{2} \mu_{N_2} = \mu_{\text{NH}_3} - \frac{3}{2} \mu_{\text{H}_2}$$

If the standard states refer to unit pressure and if ideal gases or constant fugacity coefficients can be assumed, the following holds:

$$\mu_{N,g} = \frac{1}{2} G_{N_2}^\circ + \frac{1}{2} RT \ln p_{N_2} = G_{\text{NH}_3}^\circ - \frac{3}{2} G_{\text{H}_2}^\circ + RT \ln r_N \quad [1]$$

with

$$r_N = \frac{p_{\text{NH}_3}}{p_{\text{H}_2}^{3/2}}$$

where G_j refers to the Gibbs free energy per mole of j , p_j refers to the partial pressure of j , the superscript \circ indicates the standard state of the component concerned, r_N is the so-called nitriding potential, and R and T have their usual meanings. The virtual partial pressure of N₂ corresponding to an NH₃/H₂ mixture can be calculated from Eq. [1].

If equilibrium is attained between an imposed NH₃/H₂ mixture and an Fe-N phase, the chemical potential of nitrogen in the solid Fe-N phase s ($=\alpha, \gamma', \varepsilon$) is equal to that in the gas phase: $\mu_{N,s} = \mu_{N,g}$. By variation of the composition of the NH₃/H₂ gas mixture at a certain temperature and determination of the equilibrium nitrogen content in the Fe-N phase, a nitrogen-absorption isotherm is obtained. Thereby, through Eq. [1], the chemical potential of nitrogen in an Fe-N phase can be determined experimentally as a function of the nitrogen content. Fitting of a theoretical description for the chemical potential to the experimental nitrogen-absorption isotherm data provides values for the unknown parameters in this description.

A. α -Fe

For nitrogen in ferrite, a regular solution of nitrogen on its own sublattice can be assumed. The nitrogen content on the interstitial sublattice is so low that excess enthalpy does not have to be taken into account. Hence, the chemical potential of nitrogen in ferrite, $\mu_{N,\alpha}$, is

$$\mu_{N,\alpha} = G_{N,\alpha}^\circ + RT \ln \left[\frac{y_{N,\alpha}}{1 - y_{N,\alpha}} \right] \quad [2]$$

with $y_{N,\alpha}$ as the fraction of interstitial sites occupied by N atoms. For equilibrium with an ammonia/hydrogen mixture, equating Eqs. [1] and [2] yields an expression for the nitrogen-absorption isotherm:

$$\frac{y_{N,\alpha}}{1 - y_{N,\alpha}} = \frac{r_N}{r_{N,\alpha}^\circ} \quad [3]$$

with $r_{N,\alpha}^\circ$ defined as $RT \ln r_{N,\alpha}^\circ = G_{N,\alpha}^\circ - G_{\text{NH}_3}^\circ + 3G_{\text{H}_2}^\circ/2$. It follows from Eq. [3] that $r_{N,\alpha}^\circ$ can be interpreted as the nitriding potential in equilibrium with ferrite of the hypothetical composition Fe₂N₃ ($y_{N,\alpha} = 1/2$; three interstitial sites per Fe site in bcc Fe). Since $y_{N,\alpha}$ is very small (maximally $1.339 \cdot 10^{-3}$ at 863 K⁽²¹⁾), the denominator in Eq. [3] can be replaced by 1. From an evaluation of literature data, the following was found for the temperature dependence of the nitrogen-absorption isotherms of α -Fe ($573 \text{ K} < T < 863 \text{ K}$; see Appendix)

$$\ln r_{N,\alpha}^\circ = -\ln \left[y_{N,\alpha} \cdot \frac{1}{r_N} \right] = -11.56 + \frac{9096}{T} \quad [4]$$

where r_N is given in Pa^{-1/2} and T is given in kelvin.

B. γ' -Fe₄N_{1-x}

Long-range ordering of N atoms in γ' -Fe₄N_{1-x} implies that these atoms prefer to occupy one of the four octahedral interstices in the fcc unit cell of the Fe atoms (order sites). To arrive at an accurate description of the available experimental data for the nitrogen-absorption isotherms of γ' -Fe₄N_{1-x}, it was shown necessary to take into account the (very low) occupancy by N atoms of the other, not preferred, octahedral interstices (disorder sites⁽¹²⁾) as well. The chemical potential of nitrogen in γ' -nitride, $\mu_{N,\gamma'}$, can be described as a function of nitrogen content and temperature with the same accuracy by a GBW approach and a Wagner-Schottky (WS) approach, as was shown in Reference 12. The WS approach is more convenient mathematically than the GBW approach and it is therefore adopted here:

$$\mu_{N,\gamma'} = G_{N,\gamma'}^\circ + RT \ln \left\{ \sqrt{1 + \left(\frac{\Delta y_{N,\gamma'}}{2K_{\gamma'}} \right)^2} + \frac{\Delta y_{N,\gamma'}}{2K_{\gamma'}} \right\} \quad [5]$$

where $4\Delta y_{N,\gamma'} = 4y_{N,\gamma'} - 1$, with $y_{N,\gamma'}$ as the fraction of the interstitial sublattice occupied by N atoms, describes the deviation of the composition from the stoichiometry Fe₄N(Fe₄N_{1+4\Delta y_{N,\gamma'}}) and $16/3 (K_{\gamma'})^2$ is the equilibrium constant for the exchange of nitrogen atoms at order sites with nitrogen atoms at disorder sites. For equilibrium with an ammonia/hydrogen mixture, equating Eqs. [1] and [5] yields an expression for the nitrogen-absorption isotherm:

$$\frac{r_N}{r_{N,\gamma'}^\circ} = \left\{ \sqrt{1 + \left(\frac{\Delta y_{N,\gamma'}}{2K_{\gamma'}} \right)^2} + \frac{\Delta y_{N,\gamma'}}{2K_{\gamma'}} \right\} \quad [6]$$

with $r_{N,\gamma'}^\circ$ defined as $RT \ln r_{N,\gamma'}^\circ = G_{N,\gamma'}^\circ - G_{\text{NH}_3}^\circ + 3G_{\text{H}_2}^\circ/2$. It follows from Eq. [6] that $r_{N,\gamma'}^\circ$ can be interpreted as the nitriding potential in equilibrium with γ' -Fe₄N_{1-x} of the hypothetical composition Fe₄N₁ ($y_{N,\gamma'} = 1/4$; one interstitial site per Fe site in fcc Fe). According to Reference

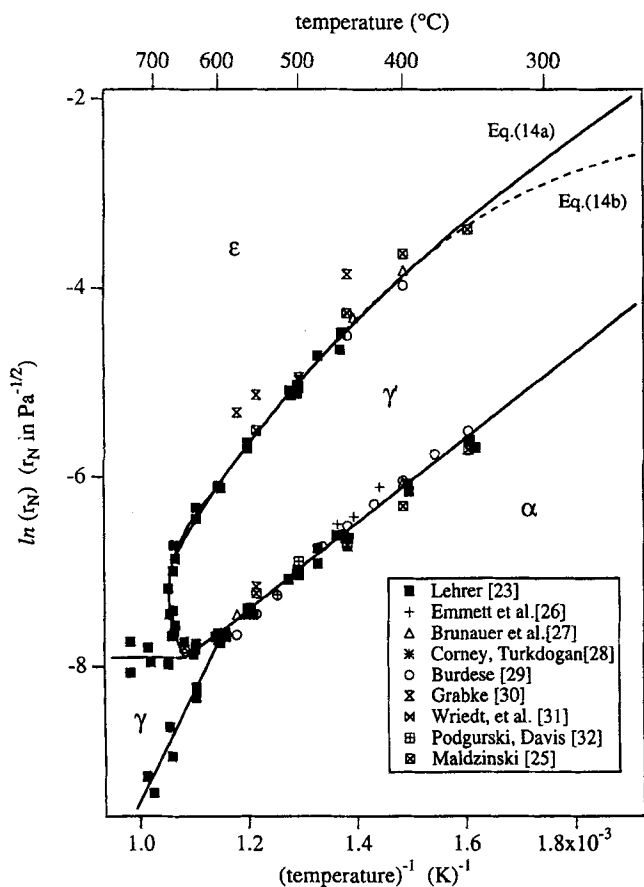


Fig. 1—Lehrer diagram, showing the nitriding-potential ranges of the Fe-N phases: the nitriding potential, r_N , at the phase boundaries is given as a function of the temperature, T . Analytical expressions for the boundaries between the α -Fe and γ -Fe₄N_{1-x} phase fields and the γ -Fe₄N_{1-x} and ϵ -Fe₂N_{1-z} phase fields are given by Eqs. [13] and [14], respectively. The dashed line corresponds to Eq. [14b], to be distinguished from the solid line corresponding to Eq. [14a] only for $T < 673$ K. The experimental data from Ref. 23 determine a phase boundary as an intermediate between data indicating the periphery of the associated phase fields.

12, the values for $r_{N,\gamma}^\circ$ and K_γ are given by

$$\ln r_{N,\gamma}^\circ = -12.5 + \frac{6.35 \cdot 10^3}{T} \quad [7a]$$

$$\ln 4K_\gamma = 2.98 - \frac{7.56 \cdot 10^3}{T} \quad [7b]$$

where $r_{N,\gamma}^\circ$ is given in Pa^{-1/2} and T is given in kelvin.

C. ϵ -Fe₂N_{1-z}

Long-range ordering of N atoms in ϵ -Fe₂N_{1-z} can be described on the basis of a simple hexagonal unit cell for the interstitial sublattice containing six types of sites (A1, B1, C1, A2, B2, C2), which represent six sublattices for the nitrogen atoms. The GBW approach^[22] was applied to the interstitial sublattice occupied by N atoms and V atoms (vacancies).^[11] The interaction among the atoms was accounted for by an exchange energy $W_{N,\epsilon}^c$ representing pairwise interaction in the direction perpendicular to the basal plane of the hexagonal unit cell (sites denoted by the same character A, B, or C) and an exchange energy $W_{N,\epsilon}^p$ representing the pairwise interactions in the basal plane of the hexagonal unit cell (sites denoted by the same number 1 or

2). On this basis, a very good description of the chemical potential of nitrogen in ϵ -Fe₂N_{1-z} as a function of nitrogen content and temperature was obtained in Reference 13. For the chemical potential of interstitials at sites of type A1, ${}^{A1}\mu_{N,\epsilon}$ the following holds.^[13]

$${}^{A1}\mu_{N,\epsilon} = G_{N,\epsilon}^\circ + RT \ln \left[\frac{{}^{A1}y_{N,\epsilon}}{1 - {}^{A1}y_{N,\epsilon}} \right] + \quad [8]$$

$$\left(1 - 2 {}^{A2}y_{N,\epsilon} \right) W_{N,\epsilon}^c + \left(1 - {}^{B1}y_{N,\epsilon} + {}^{C1}y_{N,\epsilon} \right) W_{N,\epsilon}^p$$

where ${}^k y_{N,\epsilon}$ is the fraction of sites of type k occupied by N atoms. Analogous equations hold for the chemical potentials of the interstitials at the other types of sites. At equilibrium, the six chemical potentials are equal. For equilibrium with an ammonia/hydrogen mixture, equating Eqs. [1] and [8] yields

$$\ln \frac{r_N}{r_{N,\epsilon}^\circ} = \ln \left[\frac{{}^{A1}y_{N,\epsilon}}{1 - {}^{A1}y_{N,\epsilon}} \right] + \quad [9]$$

$$\left(1 - 2 {}^{A2}y_{N,\epsilon} \right) \frac{W_{N,\epsilon}^c}{RT} + \left(1 - {}^{B1}y_{N,\epsilon} - {}^{C1}y_{N,\epsilon} \right) \frac{W_{N,\epsilon}^p}{RT}$$

with $r_{N,\epsilon}^\circ$ defined as $RT \ln r_{N,\epsilon}^\circ = G_{N,\epsilon}^\circ - G_{NH_3}^\circ + 3G_{H_2}^\circ/2$. It follows from Eq. [9] that $r_{N,\epsilon}^\circ$ can be interpreted as the nitriding potential in equilibrium with ϵ -Fe₂N_{1-z} having the hypothetical composition Fe₂N and ${}^{A1}y_{N,\epsilon} = {}^{B1}y_{N,\epsilon} = {}^{C1}y_{N,\epsilon} = {}^{A2}y_{N,\epsilon} = {}^{B2}y_{N,\epsilon} = {}^{C2}y_{N,\epsilon} = 1/2$ (i.e., a random distribution of N atoms over all available sites; one interstitial site per Fe atom in hcp Fe). Analogous equations hold for the other types of sites. Values for ${}^k y_{N,\epsilon}$ can be obtained numerically from the set of six equations of type Eq. [9] (refer to References 11 and 13 for numerical recipes). Two solutions pertaining to distinct ordered configurations of the N atoms, denoted A and B, were found for exchange energies $W_{N,\epsilon}^p/RT < 0$ and $W_{N,\epsilon}^c/RT < 0$, implying mutual repulsion among N atoms. Configuration B is the most stable one for compositions near Fe₂N_{2/3}; configuration A is the most stable one for the higher nitrogen contents, up to Fe₂N.^[11]

From fitting the GBW model to experimental data for nitrogen-absorption isotherms of ϵ -Fe₂N_{1-z}, it was concluded in Reference 13 that, within the composition range Fe₃N to Fe₂N and temperature range 673 to 823 K investigated, configuration A is dominant and that the exchange energies can be taken directly proportional to the temperature. However, the nitrogen contents of ϵ -Fe₂N_{1-z} which are of importance for calculation of the $\gamma'/(\gamma' + \epsilon)$ and $(\gamma' + \epsilon)/\epsilon$ phase boundaries are generally near or below that for Fe₃N. For these compositions, it was shown in Reference 13 that (1) configuration B is more stable than configuration A and (2) the parameters $W_{N,\epsilon}^p$, $W_{N,\epsilon}^c$ and $\ln r_{N,\epsilon}^\circ$ obtained for configuration A apply to configuration B as well. Hence, for calculation of the $(\gamma' + \epsilon)/\epsilon$ phase boundary, configuration B has to be adopted for the ϵ phase using the following values for the exchange energies:^[13]

$$\frac{W_{N,\epsilon}^p}{RT} = -4.48, \quad \frac{W_{N,\epsilon}^c}{RT} = -2.98 \quad [10a]$$

and for the reference nitriding potential $r_{N,\epsilon}^\circ$.^[13]

$$\ln r_{N,\epsilon}^{\circ} = -4.92 + \frac{3.59 \cdot 10^3}{T} \quad [10b]$$

where $r_{N,\epsilon}^{\circ}$ is given in $\text{Pa}^{-1/2}$ and T in kelvin.

Instead of using the set of equations of type Eq. [9] with parameter values given by Eq. [10] for the calculation of the phase boundaries, a more convenient analytical description relating the total occupancy of the nitrogen sublattice,

$$y_{N,\epsilon} = 1 \sum_{k=A1}^{C2} k y_{N,\epsilon} / 6, \text{ to the nitriding potential, } r_{N,\epsilon}, \text{ is desired.}$$

It was found that the following equations provide an adequate description of the set of equations of type Eq. [9] using the values determined for $W_{N,\epsilon}^p/RT$ and $W_{N,\epsilon}^c/RT$ (Eq. [10a]) for specific $y_{N,\epsilon}$ ranges:

$$0.26 < y_{N,\epsilon} < 0.37: \ln \left(\frac{r_{N,\epsilon}}{r_{N,\epsilon}^{\circ}} \right) = -3.84 - 30.76 y_{N,\epsilon} + 82.87 (y_{N,\epsilon})^2 \quad [11a]$$

$$0.16 < y_{N,\epsilon} < 0.26: \ln \left(\frac{r_{N,\epsilon}}{r_{N,\epsilon}^{\circ}} \right) = -8.61 + 5.03 y_{N,\epsilon} + 15.60 (y_{N,\epsilon})^2 \quad [11b]$$

where $r_{N,\epsilon}^{\circ}$ is still given by Eq. [10b]. Note that Eq. [11], in particular Eq. [11b], is obtained by severe extrapolation of Eq. [9] using the values of Eq. [10], because Eq. [10] holds for the composition range $0.36 < y_{N,\epsilon} < 0.50$.

III. EQUILIBRIUM BETWEEN FE-N PHASES; CALCULATION OF PHASE BOUNDARIES IN THE FE-N SYSTEM

Equilibrium between two phases is established if the chemical potentials of each of the composing elements are the same in both phases. Hence, for equilibrium between $\alpha\text{-Fe[N]}$ and $\gamma\text{-Fe}_4\text{N}_{1-x}$,

$$\mu_{N,\alpha} = \mu_{N,\gamma'} \text{ and } \mu_{\text{Fe},\alpha} = \mu_{\text{Fe},\gamma'} \quad [12]$$

If, as a function of composition and temperature for both phases, the Gibbs free energy and thus the chemical potentials of nitrogen and iron are known, then the phase boundaries $\alpha/\alpha + \gamma'$ and $\alpha + \gamma'/\gamma'$ can be calculated straightforwardly by application of Eq. [12]. The chemical potential of dissolved nitrogen (or *via* Eq. [1] the corresponding nitriding potential) as a function of composition and temperature was derived in Section II for each of the three phases $\alpha\text{-Fe[N]}$, $\gamma'\text{-Fe}_4\text{N}_{1-x}$, and $\epsilon\text{-Fe}_2\text{N}_{1-x}$. The values for $G_{N,s}^{\circ}$ ($G_{N,s}^{\circ} = RT \ln r_{N,s}^{\circ} + G_{\text{NH}_3}^{\circ} - 3G_{\text{H}_2}^{\circ}/2$, where $s = \alpha, \gamma', \epsilon$) are determined on the basis of the experimental values for $r_{N,s}^{\circ}$ (section II). Then, the chemical potentials of iron, $\mu_{\text{Fe},s}$, can be obtained from

$$G_s = \frac{a}{c} \mu_{\text{Fe},s} + y \mu_{N,s}$$

where G_s is the Gibbs free energy for an amount of phase s ($=\alpha, \gamma', \epsilon$) corresponding with a/c mol Fe atoms and y mol N atoms, and a/c denotes the number of Fe sites with respect to the number of interstitial sites available for N

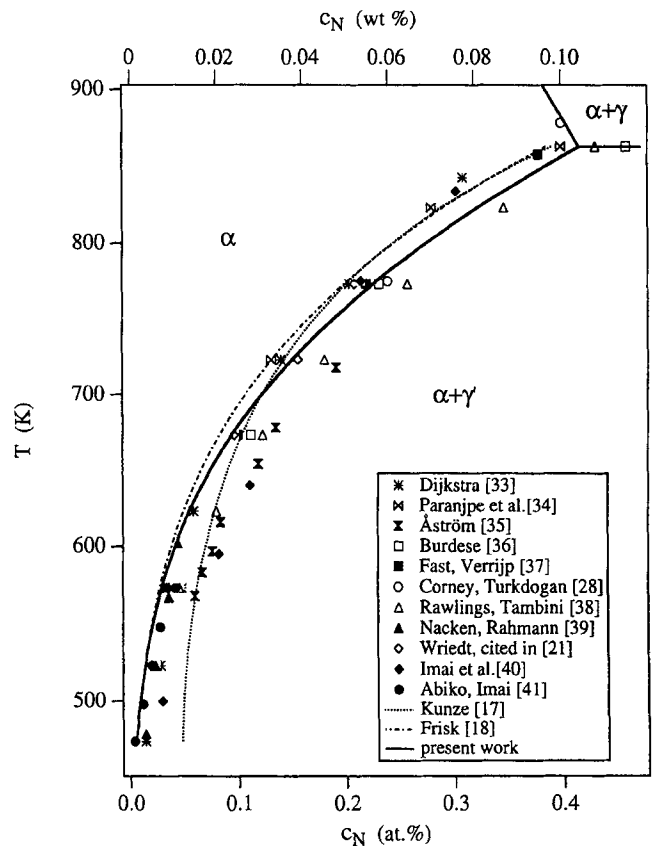


Fig. 2—Part of the Fe-N phase diagram, temperature T vs the nitrogen content c_N , showing the $\alpha/\alpha + \gamma$ phase boundary: the $\alpha/\alpha + \gamma$ phase boundary as calculated in the present work (solid line) and those proposed in Ref. 17 (dotted line) and Ref. 18 (dash-dot line), and the corresponding experimental data.

atoms (e.g., $a/c = 1/3$ for $\alpha\text{-Fe}$). The only unknowns are the values for $G_{\text{Fe},s}^{\circ}$. No experimental data for the direct evaluation of $G_{\text{Fe},\gamma'}^{\circ}$ and $G_{\text{Fe},\epsilon}^{\circ}$ with respect to some reference (e.g., $G_{\text{Fe},\alpha}^{\circ}$) are available. For this reason, in previous calculations of the Fe-N phase diagram,^[14-20] experimental composition-temperature data of the Fe-N phase diagram were used in order to evaluate (by fitting) the unknown parameters in the description of the Gibbs free energy. Then, depending on the number of composition-temperature data used, a comparison of the calculated and the experimentally assessed phase diagrams may lose its potentially vindicating significance and a (seemingly) correct Fe-N phase diagram can be calculated, although its underlying thermodynamic description is wrong. In the present work, another route is followed in which use of experimental composition-temperature data of the Fe-N phase diagram is circumvented. Here, the nitriding potential (cf. Eq. [1]) holding for equilibrium between a NH_3/H_2 mixture and two coexisting iron-nitrogen phases was used. In the following, these nitriding potentials will be denoted as phase-boundary nitriding potentials $r_{N,i/j}$, with i and j as the coexisting phases. The $r_{N,i/j}$'s are experimentally well established and are presented in a so-called Lehrer diagram,^[23] depicting the nitriding-potential ranges of the Fe-N phases in a plot of the composition of the ammonia/hydrogen mixture vs temperature (Figure 1). The description of the phase boundaries can be obtained directly by substitution of the

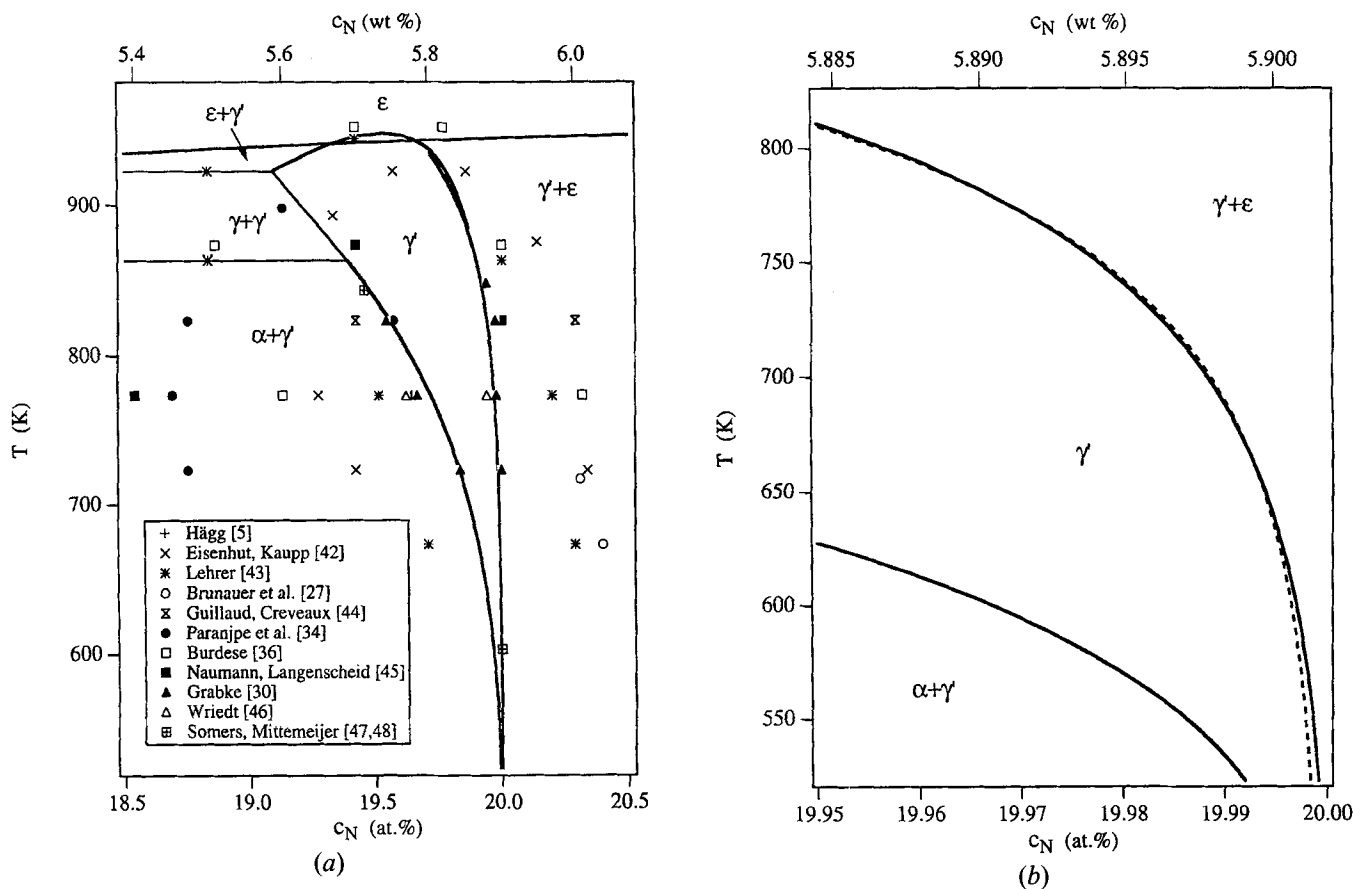


Fig. 3—(a) and (b) Part of the Fe-N phase diagram, temperature T vs the nitrogen content c_N , showing the γ - Fe_4N_{1-x} homogeneity range: the $\alpha + \gamma'$ and $\gamma/\gamma' + \epsilon$ phase boundaries as calculated in the present work (bold lines) and the corresponding experimental data. Enlargement of γ -phase field in (b) shows that using either Eq. [14a] (solid line) or Eq. [14b] (dashed line) does not have a significant effect on the $\gamma/\gamma' + \epsilon$ phase boundary.

$r_{N,i/j}$'s in the descriptions of the absorption isotherms for each phase, as derived in Section II.

A. Coexisting α -Fe and γ' - Fe_4N_{1-x} in Equilibrium with NH_3/H_2 Mixtures

Using the original data of Reference 23, the additional data of the compilation provided in Reference 21* and the

*In the compilation of Ref. 21 also, the data of Ref. 23 appear to have been incorporated. However, instead of using the original experimental data, the "data points" given in Ref. 21 were derived from a (fitted) line.

data of References 24 and 25, the temperature dependence of the phase-boundary nitriding potential for coexisting α -Fe and γ' - Fe_4N_{1-x} , $r_{N,\alpha/\gamma'}$, can be represented by the following relation obtained by linear regression (Figure 1):

$$\ln r_{N,\alpha/\gamma'} = \frac{4555}{T} - 12.88 \quad [13]$$

with $r_{N,\alpha/\gamma'}$ in $Pa^{-1/2}$ and T in Kelvin. Substitution of r_N in Eq. [4] by $r_{N,\alpha/\gamma'}$ as given by Eq. [13], yields the $\alpha/\alpha + \gamma'$ phase boundary. The resulting phase boundary is given in Figure 2 by the solid line and can be compared in this figure with the experimental data for the $\alpha/\alpha + \gamma'$ phase boundary as well as the calculated $\alpha/\alpha + \gamma'$ phase boundaries given in recent evaluations of the Fe-N phase diagram.^[17,18] The agreement of the present description for the

phase boundary and the experimental data is good, especially with the data of Reference 37 given for the entire temperature range and the data of References 39 and 41 which are available only for relatively low temperatures. Only the data of Reference 35 in general and the data of Reference 40 at low temperatures deviate significantly; these suggest a considerably higher solubility of nitrogen in α than predicted here. In this respect, it is remarked that the experimentally determined nitrogen contents for the $\alpha/\alpha + \gamma'$ phase boundary tend to be too high due to the un-noticed presence of finely dispersed γ' - Fe_4N_{1-x} or α'' - $Fe_{16}N_2$ precipitates in α -Fe.^[37] Indeed, it has been shown in Reference 37 that such a systematic error is likely to have influenced considerably the data of Reference 35. Also in Reference 21, on the basis of an evaluation of all data for the $\alpha/\alpha + \gamma'$ phase boundary, the data of Reference 37 were recommended as most reliable ($T > 573$ K).

The present calculation of the $\alpha/\alpha + \gamma'$ phase boundary does not use explicitly phase-boundary data as in References 14 through 20 (refer to preceding discussion). In the calculations presented in References 14 through 18, equilibrium was considered between α -Fe[N] and a phase with the stoichiometric composition Fe_4N or $Fe_{4.1}N$ ($Fe_{4.15}N$, $Fe_{4.3}N$). Because the chemical potential of nitrogen in γ' phase is very sensitive to small variations in the nitrogen content, the results obtained for the $\alpha/\alpha + \gamma'$ phase boundary in References 14 through 18 on the basis of these hy-

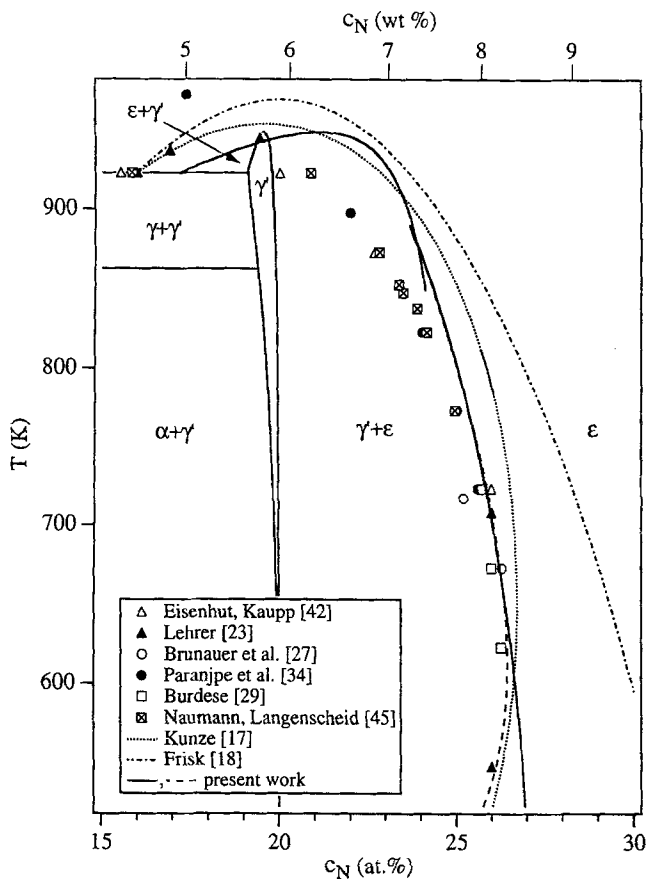


Fig. 4—Part of the Fe-N phase diagram, temperature T vs the nitrogen content c_N , showing the $\gamma' + \epsilon/\epsilon$ phase boundary: the $\gamma' + \epsilon/\epsilon$ phase boundary as calculated in the present work (bold solid and bold dashed lines for which Eqs. [14a] and [14b] are used, respectively) and as proposed in Ref. 17 (dotted line) and in Ref. 18 (dash-dot line), and the corresponding experimental data.

pothetical equilibria are only approximate. Further, in Reference 12, it was shown that ignoring the occurrence of long-range ordering of N atoms in γ' phase, as was done in References 19 and 20, led to an incorrect description of the thermodynamics of this phase. Nevertheless, the $\alpha/\alpha + \gamma'$ phase boundary, as obtained in References 19 and 20, compares favorably with the corresponding experimental data. This good agreement should be attributed to using explicitly phase-boundary data for the "calculation" of the phase boundary.

Substitution of r_N in Eq. [6] by $r_{N,\alpha/\gamma'}$, as given by Eq. [13] and using Eq. [7], yields the $\alpha + \gamma'/\gamma'$ phase boundary. The resulting phase boundary is given in Figure 3(a) and can be compared in this figure with the experimental data for this phase boundary. Clearly, the experimental composition-temperature data reported by different authors scatter enormously. The discrepancies can be ascribed to experimental difficulties in determining the nitrogen contents in γ' -nitride for the α/γ' two-phase equilibrium, as holds especially for the older references. For a discussion of the possible experimental difficulties, see Reference 49. Minute changes in the nitrogen content in γ' correspond with large changes of the corresponding nitriding potential. Changes of the $r_{N,\alpha/\gamma'}$ can be obtained with a relatively

high accuracy. Therefore, it is believed that the present phase boundary calculated by combining nitrogen-absorption isotherms for γ' -nitride and phase-boundary nitriding potentials for the α/γ' equilibrium is much more accurate than the experimental composition data for this phase boundary.

B. Coexisting γ' - Fe_4N_{1-x} and ϵ - Fe_2N_{1-z} in Equilibrium with NH_3/H_2 Mixtures

Using the original data of Reference 23, the additional data of the compilation provided in Reference 21 (from Reference 30 incorporated in Reference 21, only those at 773 K; outliers in Figure 1), and the data of References 24 and 25, the temperature dependence of the phase boundary nitriding potential, $r_{N,\gamma'/\epsilon}$, for coexisting γ' - Fe_4N_{1-x} and ϵ - Fe_2N_{1-z} , $r_{N,\gamma'/\epsilon}$ is obtained by least-squares fitting as follows (Figure 1).

for $623 \text{ K} < T < 900 \text{ K}$:

$$\ln r_{N,\gamma'/\epsilon} = -9.63 + \sqrt{\frac{60,536}{T} - 56.85} \quad [14a]$$

or, with comparable accuracy:

$$\ln r_{N,\gamma'/\epsilon} = -\left(\frac{2150}{T}\right)^2 + \frac{18,708}{T} - 21.46 \quad [14b]$$

and for $T > 870 \text{ K}$:

$$\ln r_{N,\gamma'/\epsilon} = -7.26 \pm \sqrt{\frac{14,385}{T} - 15.16} \quad [14c]$$

with $r_{N,\gamma'/\epsilon}$ in $\text{Pa}^{-1/2}$ and T in kelvin. Substitution of r_N in Eq. [6] by $r_{N,\gamma'/\epsilon}$ as given by Eq. [14], also using Eq. [7], yields the $\gamma'/\gamma' + \epsilon$ phase boundary. The result is depicted in Figure 3(a) and can be compared in this figure with the experimental data for this phase boundary. For comparison of the calculated phase boundary with the experimental data, the same considerations apply as for the $\alpha + \gamma'/\gamma'$ phase boundary. The composition corresponding with the congruent equilibrium $\gamma' \rightleftharpoons \epsilon$ at $T = 949 \text{ K}$ (this temperature follows directly from Eq. [14c] by taking the square root term equal to zero) was calculated to be 19.53 at. pct N. This calculated content is in excellent agreement with the results reported in References 27 and 38. An evaluation in Reference 21 yielded as most probable composition and temperature for this congruent reaction 19.5 at. pct N at 953 K. Taking either Eq. [14a] or Eq. [14b] for $r_{N,\gamma'/\epsilon}$ at $T < 900 \text{ K}$ yields a minor difference in the calculated results for the $\gamma'/\gamma' + \epsilon$ phase boundary: a difference of only 0.007 at. pct N at 523 K (Figure 3(b)). Apparently, the calculated phase boundary is not sensitive to small deviations of the value for $r_{N,\gamma'/\epsilon}$. Hence, it is anticipated that the $\gamma'/\gamma' + \epsilon$ phase boundary, as calculated from the experimentally determined phase-boundary nitriding potential $r_{N,\gamma'/\epsilon}$ will be more accurate than the experimentally determined nitrogen contents for the $\gamma'/\gamma' + \epsilon$ phase boundary.

Substitution of r_N in Eq. [11] by $r_{N,\gamma'/\epsilon}$ as given by Eq. [14], also using Eq. [10b], yields the $\gamma' + \epsilon/\epsilon$ phase boundary. The result is depicted in Figure 4 and can be compared in this figure with the experimental data for this phase

boundary* as well as with the previously calculated (cf.

*The experimental compositions pertaining to the $\gamma' + \varepsilon/\varepsilon$ phase boundary in the temperature range 523 K < T < 900 K can be described by (least-squares fitting)

$$\frac{y_{N,\varepsilon}}{1 + y_{N,\varepsilon}} = 5.758 \times 10^{-2} + 6.621 \times 10^{-4} T - 5.345 \times 10^{-7} T^2$$

, where T is the temperature in kelvin.

discussion in the beginning of this section) $\gamma' + \varepsilon/\varepsilon$ phase boundaries, as given in References 17 and 18. As compared to the previously calculated $\gamma' + \varepsilon/\varepsilon$ phase boundaries in References 14 through 20, the one obtained here agrees much better with the available experimental data in the temperature range 600 through 800 K. Furthermore, in contrast with the previous calculations, experimental data from the phase diagram were not used in the present prediction of the phase diagram. At higher temperatures, the calculated $\gamma' + \varepsilon/\varepsilon$ phase boundary deviates significantly from the experimental data for the $\gamma' + \varepsilon/\varepsilon$ phase boundary, resulting in a calculated composition for the congruent equilibrium $\gamma' \rightleftharpoons \varepsilon$ of 21.2 at. pct N, which is about 1.7 at. pct N too high. In this respect, the present result only seems less good than the results of References 14 through 20: it should be recognized that in these previous calculations, the composition and temperature of the congruent equilibrium $\gamma' \rightleftharpoons \varepsilon$ were fixed at their correct values *a priori*.

The discrepancy between the calculated $\gamma' + \varepsilon/\varepsilon$ phase boundary in the present work and the experimental data at temperatures higher than 800 K probably originates from the restricting adoption that $W_{N,\varepsilon}^p/RT$ and $W_{N,\varepsilon}^c/RT$ are constant. Adopting $W_{N,\varepsilon}^p/RT$ and $W_{N,\varepsilon}^c/RT$ as constants led to a good fit of the GBW model to the experimental absorption-isotherm data in the temperature range 673 to 723 K (Reference 13) and, indeed, the $\gamma' + \varepsilon/\varepsilon$ phase boundary is very well described in this temperature range. No reliable absorption-isotherm data exist for temperatures above about 723 K. As shown in Reference 13, this is due to the occurrence of a stationary state, rather than equilibrium, at the gas/ ε -phase interface. Therefore, it is impossible to provide a more detailed description of the temperature dependence of the exchange energies, although it is recognized that the predicted phase boundary strongly depends on this temperature dependence. For example, if $W_{N,\varepsilon}^p$ and $W_{N,\varepsilon}^c$ are taken as constants, which can be obtained from fitting the same GBW model to the absorption-isotherm data in the temperature range 673 to 723 K (Reference 13), the calculated $\gamma' + \varepsilon/\varepsilon$ phase boundary at the higher temperatures strongly deviates from the experimental data in the opposite direction (*i.e.*, it is situated at too low nitrogen contents). Therefore, it is suggested that $W_{N,\varepsilon}^p/RT$ and $W_{N,\varepsilon}^c/RT$ described with the form $a + b/T$ provide a temperature dependence in-between the two considered in Reference 13 and may provide a description of the $\gamma' + \varepsilon/\varepsilon$ phase boundary that is in better agreement with the experimental phase-boundary data than the one calculated here.

Taking either Eq. [14a] or Eq. [14b] for $r_{N,\gamma'/\varepsilon}$ both valid for 623 K < T < 900 K, yields distinctly different $\gamma' + \varepsilon/\varepsilon$ phase boundaries at temperatures below about 650 K: the difference in nitrogen content amounts to about 1 at. pct N if the range of applications of Eqs. [14a] and [14b] is extended to 523 K (Figure 4). Evidently, the calculated $\gamma' + \varepsilon/\varepsilon$ phase boundary, unlike the calculated $\gamma'/\gamma' + \varepsilon$ phase boundary in this temperature range (compare Figures

3(b) and 4 and refer to previous discussion), is very sensitive to small changes in the value for $r_{N,\gamma'/\varepsilon}$. This implies that a small, seemingly insignificant, systematic inaccuracy in the description of $r_{N,\gamma'/\varepsilon}$ or in the description of the absorption isotherm close to the phase boundary under consideration can cause a significant error in the calculated composition of ε in equilibrium with γ' . In this respect, it is noted that in the calculation of the $\gamma' + \varepsilon/\varepsilon$ phase boundary, the relevant part of the nitrogen-absorption isotherms for ε is that at low nitrogen content, where the number of data is limited and thus the fit relies largely on the data at higher nitrogen contents.

C. Coexisting α -Fe and ε -Fe₂N_{1-z} in Equilibrium with NH₃/H₂ Mixtures

For the temperature range pertaining to the Lehrer diagram (Figure 1), no equilibrium can occur between a gas mixture of ammonia and hydrogen (or, equivalently, pure nitrogen gas with the pressure corresponding with the partial pressure of the ammonia/hydrogen mixture) and coexisting solid phases α -Fe and ε -Fe₂N_{1-z}. A possible equilibrium of the α and ε phases implies that the phase-boundary nitriding potentials $r_{N,\alpha/\gamma'}$ and $r_{N,\gamma'/\varepsilon}$ attain a certain, identical value at a certain temperature: a triple point where α , γ' , and ε coexist. Equating Eqs. [13] and [14a] yields for the temperature of the triple point 295.4 K, which gives, with Eq. [11], for the composition of ε -nitride at the triple point $y_{N,\varepsilon} = 0.341$; equating Eqs. [13] and [14b] yields for the temperature of the triple point 448.6 K, which gives, with Eq. [11], for the composition of ε -nitride at the triple point $y_{N,\varepsilon} = 0.288$. Both Eqs. [14a] and [14b] are equally justified least-squares fits to the same experimental data. The distinct predictions for the triple point on extrapolation to low temperatures are the result of the adopted empirical functional dependence of $r_{N,\gamma'/\varepsilon}$ on $1/T$. Therefore, no conclusion can be drawn regarding the temperature of an $\alpha/\gamma'/\varepsilon$ triple point on the basis of the present data.

Recently, the observation that γ' -nitride did not appear on annealing an ε -nitride layer (produced by 1 MeV implantation of N⁺ into iron and, consequently, buried in a ferrite substrate*) at T < 573 K was taken as an experi-

*In general, experiments on iron-nitrogen phases obtained by ion-beam implantation cannot be related easily to the equilibrium conditions pertaining to the (common) Fe-N phase diagram. Equilibrium should be established between a homogeneous Fe-N phase and an ammonia/hydrogen gas mixture or, equivalently, nitrogen gas of corresponding high partial pressure. Without imposing such high (virtual) partial pressures of nitrogen, approaching thermodynamic equilibrium for as-produced Fe-N phases invariably leads to a decomposition into N₂ and ferrite with a low nitrogen content (or austenite at higher temperature), provided N atoms can recombine at favorable sites.

mental indication that, in the usual Fe-N phase diagram at temperatures lower than 573 K, the γ' phase field would vanish.^[50,51] This conclusion was further substantiated by experiments with two-phase ε/γ' samples where the γ' phase could be transformed into ε -nitride containing about 20 at. pct N (the same composition as the parent γ' -nitride) at temperatures as low as 423 K, provided a beam of Ne⁺ ions traversed the sample during the transformation. Annealing the samples in which γ' phase had been transformed into ε phase at and above 423 K led to the reappearance of γ' -nitride.^[51] From this interesting obser-

vation of a "reversible" $\gamma' \rightleftharpoons \varepsilon$ transformation, the conclusion was drawn that the γ' phase is thermodynamically unstable at temperatures below 423 K. This temperature is in-between the two estimates for the triple point calculated previously.**

**With regard to the reversible $\gamma' \rightleftharpoons \varepsilon$ transformation, the work introduced into the sample by the beam of Ne^+ ions during annealing introduces displacements of both iron atoms and nitrogen atoms, which, if they were due to thermal activation, would require a higher temperature. The possible introduction of stacking faults in the iron sublattice due to ion bombardment may be locally associated with the transformation of the fcc sublattice of iron atoms to the hcp sublattice of iron atoms. The nitrogen atoms in γ' -nitride show almost perfect long-range ordering on their own sublattice,^[12] whereas the nitrogen atoms in ε -nitride are not so strongly ordered.^[13] The strong ordering of nitrogen atoms in γ' may be disturbed by ion bombardment. Both consequences of Ne^+ bombardment, viz. the introduction of stacking faults and the disordering of the nitrogen atoms, may favor the formation of ε -nitride from γ' -nitride.

IV. CONCLUSIONS

Experimental nitrogen-absorption isotherms of the α -Fe[N], γ' - $\text{Fe}_4\text{N}_{1-x}$, and ε - $\text{Fe}_2\text{N}_{1-z}$ phases were described accurately by adopting thermodynamic models for these phases according to a regular interstitial solution, the WS approach, and a GBW approach, respectively. The $\alpha/\alpha + \gamma'$, $\alpha + \gamma'/\gamma'$, $\gamma'/\gamma' + \varepsilon$, and $\gamma' + \varepsilon/\varepsilon$ phase boundaries were calculated by substituting the nitriding potentials pertaining to the α/γ' and γ'/ε two-phase equilibria in the theoretical descriptions of the absorption isotherms. The calculated phase boundaries agree very well with the most reliable experimental data. In particular, the calculated $\gamma' + \varepsilon/\varepsilon$ phase boundary provides a major improvement as compared to earlier results. The $\gamma' + \varepsilon/\varepsilon$ phase boundary was found to be very sensitive at relatively low temperature (<650 K) to small inaccuracies in the nitriding potential pertaining to the γ'/ε two-phase equilibrium, whereas the $\gamma'/\gamma' + \varepsilon$ phase boundary was found to be very insensitive to the same inaccuracies. The present analysis of the Fe-N system suggests the occurrence of a $\alpha/\gamma'/\varepsilon$ triple point in-between 295 and 449 K.

ACKNOWLEDGMENTS

Dr. L. Maldzinski of the Poznan University of Technology (Poznan, Poland) is thanked for providing hitherto unpublished data presented in Figure 1. Dr. J. Kunze of the Institut für Festkörper-und Werkstofforschung (Dresden, Germany) is thanked for discussion. These investigations have been supported by the Foundation for Fundamental Research of Matter (FOM) and the Netherlands Technology Foundation (STW).

APPENDIX

Evaluation of nitrogen-absorption isotherms for α -Fe

Adopting a random distribution of nitrogen on its sublattice, the equilibrium content of nitrogen in ferrite at a certain temperature depends linearly on the nitriding potential of an ammonia/hydrogen gas mixture (Eq. [4]). The following results have been obtained experimentally for the equilibrium between α -Fe and NH_3/H_2 mixtures within the

temperature range 573 to 873 K:

$$\text{References 24 and 25: } \log \left[\frac{y_{\text{N},\alpha}}{r_{\text{N}}} \right] = +4.33 - \frac{3875}{T} \quad [\text{A1}]$$

$$\text{Reference 52: } \ln \left[\frac{y_{\text{N},\alpha}}{r_{\text{N}}} \right] = +10.27 - \frac{9270}{T} \quad [\text{A2}]$$

with $y_{\text{N},\alpha}$, r_{N} , and T in wt pct N, $\text{atm}^{-1/2}$, and kelvin, respectively, and

$$\text{References 21 and 53: } \log \left[\frac{y_{\text{N},\alpha}}{r_{\text{N}}} \right] = +7.49 - \frac{3950}{T} \quad [\text{A3}]$$

with $y_{\text{N},\alpha}$, r_{N} , and T in at. pct N, $\text{Pa}^{-1/2}$, and kelvin, respectively. If data for α -Fe above 873 K up to the α -Fe \rightarrow γ -Fe transformation and for δ -Fe would have been taken into account, other temperature dependencies would have been obtained (Reference 28). Recalculating the previous three descriptions, such that $y_{\text{N},\alpha}$ is expressed as the occupied fraction of the interstitial sublattice sites and that r_{N} and T are expressed in $\text{Pa}^{-1/2}$ and kelvin, the average of Eqs. [A1] and [A2] is

$$\ln \left[\frac{y_{\text{N},\alpha}}{r_{\text{N}}} \right] = +11.56 - 9096/T \quad [\text{A4}]$$

which is almost identical to Eq. [A3] after accounting for the change of units:

$$\ln \left[\frac{y_{\text{N},\alpha}}{r_{\text{N}}} \right] = +11.54 - 9095/T \quad [\text{A5}]$$

The difference between Eqs. [A4] and [A5] should be considered as irrelevant.

REFERENCES

1. *Source Book on Nitriding*, ASM, Metals Park, OH, 1977.
2. K.H. Jack: *Proc. R. Soc. London*, 1951, vol. A208, pp. 200-15.
3. N. DeCristofaro and R. Kaplow: *Metall. Trans. A.*, 1977, vol. 8A, pp. 35-44.
4. R. Bril: *Z. Kristallogr.*, 1928, vol. 69, pp. 26-34.
5. G. Hägg: *Nova Acta Reg. Soc. Sci. Upsaliensis*, 1929, vol. 7 (1), pp. 6-22.
6. S.B. Hendricks and P.B. Kosting: *Z. Kristallogr.*, 1930, vol. 74, pp. 511-33.
7. K.H. Jack: *Proc. R. Soc. London*, 1948, vol. A195, pp. 34-55.
8. K.H. Jack: *Acta Cryst.*, 1952, vol. 5, pp. 404-11.
9. N. DeCristofaro and R. Kaplow: *Metall. Trans. A.*, 1977, vol. 8A, pp. 425-30.
10. P. Rohegude and J. Foct: *Phys. Status Solidi A*, 1986, vol. 98, pp. 51-62.
11. B.J. Kooi, M.A.J. Somers, and E.J. Mittemeijer: *Metall. Mater. Trans. A*, 1994, vol. 25A, pp. 2797-2814.
12. B.J. Kooi, M.A.J. Somers, and E.J. Mittemeijer: *Metall. Trans. A*, 1996, vol. 26A, pp. XXX-XXX.
13. M.A.J. Somers, B.J. Kooi, L. Maldzinski, E.J. Mittemeijer, A.A. van der Horst, A.M. van der Kraan, and N.M. van der Pers: Delft University of Technology, Delft, unpublished research, 1994.
14. M. Hillert and M. Jarl: *Metall. Trans. A*, 1975, vol. 6A, pp. 553-59.
15. J. Ågren: *Metall. Trans. A*, 1979, vol. 10A, pp. 1847-52.
16. J. Kunze: *Steel Res.*, 1986, vol. 57 (8), pp. 361-67.

17. J. Kunze: *Nitrogen and Carbon in Iron and Steels: Thermodynamics*, Akademie Verlag, Berlin, 1990.
18. K. Frisk: *CALPHAD*, 1991, vol. 15 (1), pp. 79-106.
19. H. Du: *J. Phase Equilibria*, 1993, vol. 14, pp. 682-93.
20. A.F. Guillermet and H. Du: *Z. Metallkd.*, 1994, vol. 85, pp. 154-63.
21. H.A. Wriedt, N.A. Gokcen, and R.H. Nafziger: *Bull. Alloy Phase Diagrams*, 1987, vol. 8 (4), pp. 355-77.
22. W.S. Gorsky: *Z. Phys.*, 1928, vol. 50, p. 64; W.L. Bragg and E.J. Williams: *Proc. R. Soc. London*, 1934, vol. A145, p. 699; W.L. Bragg and E.J. Williams: *Proc. R. Soc. London*, 1935, vol. A151, p. 540; W.L. Bragg and E.J. Williams: *Proc. R. Soc. London*, 1935, vol. A152, p. 231.
23. E. Lehrer: *Z. Elektrochem.*, 1930, vol. 36 (6), pp. 383-92.
24. Z. Przylecki and L. Maldzinski: *Carbides, Nitrides and Borides*, Proc. 4th Int. Conf., Politechnika Poznanska, 1987, pp. 153-62.
25. L. Maldzinski: Ph.D. Thesis, Politechnika Poznanska, Poland, 1989 (in Polish).
26. P.H. Emmett, S.B. Hendricks, and S. Brunauer: *J. Am. Chem. Soc.*, 1930, vol. 52, pp. 1456-64.
27. S. Brunauer, M.E. Jefferson, P.H. Emmett, and S.B. Hendricks: *J. Am. Chem. Soc.*, 1931, vol. 53, pp. 1778-86.
28. N.S. Corney and E.T. Turkdogan: *J. Iron Steel Inst.*, 1955, vol. 180, pp. 344-48.
29. A. Burdese: *Ann. Chim.*, 1959, vol. 49, pp. 1873-84.
30. H.J. Grabke: *Ber. Bunsengesell. Phys. Chem.*, 1969, vol. 73 (6), pp. 596-601.
31. H.A. Wriedt, N.A. Gokcen, and R.H. Nafziger: *Binary Alloy Phase Diagrams*, ASM, Materials Park, OH, 1990, vol. 2, pp. 1728-30.
32. H.H. Podgurski and F.N. Davis: *Acta Metall.*, 1981, vol. 29, pp. 1-9.
33. L.J. Dijkstra: *Trans. AIME*, 1949, vol. 185, pp. 252-60.
34. V.G. Paranjpe, M. Cohen, M.B. Bever, and C.F. Floe: *Trans. AIME*, 1950, vol. 188, pp. 261-67.
35. H.U. Åström: *Arkiv Fysik*, 1954, vol. 8 (49), pp. 495-502.
36. A. Burdese: *Metall. Ital.*, 1955, vol. 8, pp. 357-61.
37. J.D. Fast and M.B. Verrijp: *J. Iron Steel Inst.*, 1955, vol. 180, pp. 337-43.
38. R. Rawlings and D. Tambini: *J. Iron Steel Inst.*, 1956, vol. 184, pp. 302-08.
39. M. Nacken and J. Rahmann: *Arch. Eisenhüttenwes.*, 1962, vol. 33 (2), pp. 131-40.
40. Y. Imai, T. Masumoto, and M. Sakamoto: *Sci. Rep. Res. Inst., Tohoku Univ., Ser. A*, 1968, vol. A20 (1), pp. 1-13.
41. K. Abiko and Y. Imai: *Trans. Jpn. Inst. Met.*, 1977, vol. 18, pp. 113-24.
42. O. Eisenhut and E. Kaupp: *Z. Elektrochem.*, 1930, vol. 36 (6), pp. 392-404.
43. E. Lehrer: *Z. Elektrochem.*, 1930, vol. 36 (7), pp. 460-73.
44. C. Guillaud and H. Creveaux: *Comt. Rend. Acad. Sci. Paris*, 1946, vol. 222, pp. 1170-72.
45. F.K. Naumann and G. Langenscheid: *Arch. Eisenhüttenwes.*, 1965, vol. 36 (9), pp. 677-82.
46. H.A. Wriedt: *Trans. AIME*, 1969, vol. 243, pp. 43-46.
47. M.A.J. Somers and E.J. Mittemeijer: *Metall. Trans. A*, 1990, vol. 21A, pp. 189-204.
48. M.A.J. Somers and E.J. Mittemeijer: *Metall. Trans. A*, 1990, vol. 21A, pp. 901-12.
49. M.A.J. Somers, N.M. van der Pers, D. Schalkoord, and E.J. Mittemeijer: *Metall. Trans. A*, 1989, vol. 20A, pp. 1533-39.
50. A.M. Vredenberg, C.M. Pérez-Martin, J.S. Custer, D.O. Boerma, L. de Wit, F.W. Saris, N.M. van der Pers, Th.H. de Keijser, and E.J. Mittemeijer: *J. Mater. Res.*, 1992, vol. 7 (10), pp. 2689-2712.
51. L. de Wit, Th. Weber, J.S. Custer, and F.W. Saris: *Phys. Rev. Lett.*, 1994, vol. 72, pp. 3835-38.
52. H.H. Podgurski and H.E. Knechtel: *Trans. AIME*, 1969, vol. 245, pp. 1595-1602.
53. H.J. Grabke: *Ber. Bunsengesell. Phys. Chem.*, 1968, vol. 72 (4), pp. 533-41.